

STABILITY OF AXIAL ORBITS IN ANALYTICAL GALACTIC POTENTIALS

R. SCUFLAIRE

Institut d'Astrophysique, Avenue de Coïnte 5, B-4000 Liège, Belgium

(Received 9 June 1994; accepted 23 December 1994)

Abstract. We study the stability of axial orbits in analytical galactic potentials as a function of the energy of the orbit and the ellipticity of the potential. The problem is solved by an analytical method, the validity of which is not limited to small amplitudes. The lines of neutral stability divide the parameter space in regions corresponding to different organizations of the main families of orbits in the symmetry planes.

Key words: galactic dynamics, periodic orbits, stability.

1. Introduction

The study of periodic orbits is a problem of great interest to the dynamics of galaxies. It is well-known that every stable periodic orbit is surrounded by a whole family of non-closed orbits with similar shapes and characteristics (Binney and Tremaine, 1987). Hence, the question of the stability of periodic orbits is an important one for the classification of the main families of orbits in galactic potentials. In particular, Pfenniger and de Zeeuw (1989) and Udry and Martinet (1994) have insisted on the importance of the stability of axial orbits for the construction and the shape of a triaxial model.

Several authors have considered the problem of the stability of axial orbits (Binney 1981, Goodman and Schwarzschild 1981, Magnenat 1982a, Lake and Norman 1983, de Zeeuw 1985, Robe 1987, Martinet and de Zeeuw 1988, Miralda-Escudé and Schwarzschild 1989). In most cases, this question has received only marginal interest. However, a detailed study of the stability of these orbits, if not limited to small amplitudes, is able to provide information on the appearance of other families of orbits, as will be shown in Section 5.

As the stability of an axial motion reduces to a two-dimensional problem (see Section 4.2), it is sufficient to consider two-dimensional galactic potentials. Of course, this reduction to a two-dimensional problem would not be possible in the presence of rotation. Indications on the stability of axial orbits in that case may be found in Martinet and de Zeeuw (1988) and Martinet and Udry (1990). We use two families of analytical potentials depending of a single parameter, the ellipticity of the isopotentials. The first one is the logarithmic potential of Binney (1981), which has been extensively used in galactic dynamics (Magnenat 1982, Gerhard and Binney 1985, Martinet and de Zeeuw 1988, Patsis and Zachilas 1990, Pearce

and Thomas 1991). The second one has been chosen mainly on the grounds of its simplicity. They are described in Section 2.

Davoust (1983) used the analytical method of Lindstedt-Poincaré to investigate the regular families of periodic orbits in model elliptical galaxies. We use the same method, in a much simpler context (anharmonic oscillator with one degree of freedom) as a starting point for the present work. In this way, we obtain analytical expressions describing axial motions as a function of two parameters, the energy of the movement and the ellipticity of the potential (Section 3). Then, in a way closely related to the method used in the study of Mathieu's equation, we determine the limits of stability in the parameter space (Section 4). In Section 5, our stability results are used to delineate regions corresponding to different organizations of the main families of orbits in the symmetry planes.

The use of the algebraic programming system REDUCE made possible our analytical computations. All analytical results (movement and limits of stability) could have been obtained with purely numerical procedures. We have, in fact, systematically confirmed our analytical results with numerical integrations (with programs mainly written in FORTRAN).

2. Models

We have studied two simple galactic models without figure rotation. We have chosen analytical potentials $V = V(x^2, y^2, z^2)$, symmetric with respect to the principal planes and whose equipotential surfaces are similar concentric ellipsoids.

The motion along one of the symmetry axis, let say the x -axis, is, of course, a problem with one degree of freedom. When we study the stability of this motion, we find that the equations for the y and z perturbations separate. Therefore we can consider successively the stability of the motion against a perturbation in the (x, y) plane, then against a perturbation in the (x, z) plane. That is the reason why we use a two-dimensional potential in what follows.

Our first potential is a logarithmic potential. Galactic models with logarithmic potential have a flat rotation curve outside of the core and have been extensively used. Binney and Tremaine (1987) used the following expression:

$$V(x, y) = \frac{1}{2} v_0^2 \ln(R_c^2 + x^2 + y^2/q^2), \quad (1)$$

where $q \leq 1$ defines the ellipticity of the equipotential curves, R_c is the core radius and v_0 the circular velocity at large distance from the centre when $q = 1$. Taking R_c as the unit length and R_c/v_0 as the unit time the expression of the potential simplifies to

$$V(x, y) = \frac{1}{2} \ln(1 + x^2 + y^2/q^2). \quad (2)$$

We shall refer to it as V_1 in the following.

Unfortunately, the density distribution associated with the logarithmic potential becomes unrealistic even for moderate values of q (shape of the isodensity curves, negative densities). So we have used a second analytical potential which has not this drawback. Our choice is rather arbitrary and has been essentially guided by computational facility:

$$V(x, y) = \sqrt{1 + x^2 + y^2/q^2} - 1. \quad (3)$$

The additive constant has been added only for aesthetic reasons so that the potential vanishes at the centre. This potential will be denoted V_2 in the following.

Both potentials can be expressed as

$$V(x, y) = f(u) \quad \text{with} \quad u = 1 + x^2 + y^2/q^2. \quad (4)$$

Their isopotential curves are similar concentric ellipses whose axis ratio is q . In the neighbourhood of the equilibrium position, they coincide, in first approximation, with the potential of a harmonic oscillator

$$V(x, y) = \frac{1}{2}x^2 + \frac{1}{2q^2}y^2 \quad (5)$$

with frequencies 1 and $1/q$ for an oscillation along the x -axis and along the y -axis respectively.

Usually x denotes the long axis. This convention would oblige us to study separately the motions along the long axis and along the short axis. It is easier to study both cases simultaneously, allowing q to take values greater than 1. To be more precise, when studying the motion along the y -axis, the change of variables

$$y = qx', \quad x = qy', \quad t = qt', \quad q = 1/q' \quad (6)$$

reduces the study of a y -axis orbit to the study of an x -axis orbit with the same energy in a potential whose ellipticity is $1/q$ instead of q .

3. Motion along the x -axis

The equations of motion may be written

$$\ddot{x} + 2xf'(1 + x^2 + y^2/q^2) = 0, \quad (7)$$

$$\ddot{y} + 2yf'(1 + x^2 + y^2/q^2)/q^2 = 0, \quad (8)$$

where f' is the derivative of f with respect to u . The motion along the x -axis obeys the equation

$$\ddot{x} + 2xf'(1 + x^2) = 0. \quad (9)$$

3.1. NUMERICAL COMPUTATION

To validate our analytical calculations, the problem has also been tackled by numerical methods. We use the Runge-Kutta method to integrate Equation (9). With 4096 equal steps per orbit, we obtain enough precision (we require an error less than 10^{-7} in the frequency) to test the correctness of the analytical expressions below. The error in the numerical computation is estimated by carrying out a second integration with a double number of steps.

3.2. ANALYTICAL COMPUTATION

Let us describe the analytical treatment of the problem. For clarity of the exposition, the particular expressions obtained for both potentials are given in the appendices. The equation of the motion along the x -axis reads

$$\ddot{x} + x + F(x) = 0. \quad (10)$$

We develop $F(x)$ as a power series of x . The solution $x(t)$ is then obtained by the Lindstedt-Poincaré method (see for instance the books of Nayfeh 1973 and Hayashi 1985, or the paper of Davoust 1983). We adopt the amplitude a of the motion as the parameter of the power series. At each step of the computation we impose the following initial conditions:

$$x(0) = a, \quad \dot{x}(0) = 0. \quad (11)$$

In this way, one obtains the angular frequency

$$\sigma = 1 + \sigma_1 a^2 + \sigma_2 a^4 + \sigma_3 a^6 + \sigma_4 a^8 + \dots, \quad (12)$$

and the motion

$$x(t) = a \cos \sigma t + a^3 (x_{10} \cos \sigma t + x_{11} \cos 3\sigma t) \\ + a^5 (x_{20} \cos \sigma t + x_{21} \cos 3\sigma t + x_{22} \cos 5\sigma t) + \dots \quad (13)$$

The parameter a is directly linked to the total energy E by the analytical relation

$$E = V(a, 0). \quad (14)$$

The second member of this relation, expressed as a power series contains only even powers of a . Let $\epsilon = a^2$ to simplify the writing. The relation $E = E(\epsilon)$ can be easily inverted and ϵ expressed as a power series of E . The above expressions giving σ and $x(t)$ are easily expressed as power series of E instead of a (in the case of $x(t)$, $x(t)/a$ rather than $x(t)$ is expressed as a series of ϵ or E). We have obtained these series up to the 18th power of ϵ or E . It required 13 hours of CPU-time on an IBM RISC 6000 station and the computation time doubles when the order is increased by one unit.

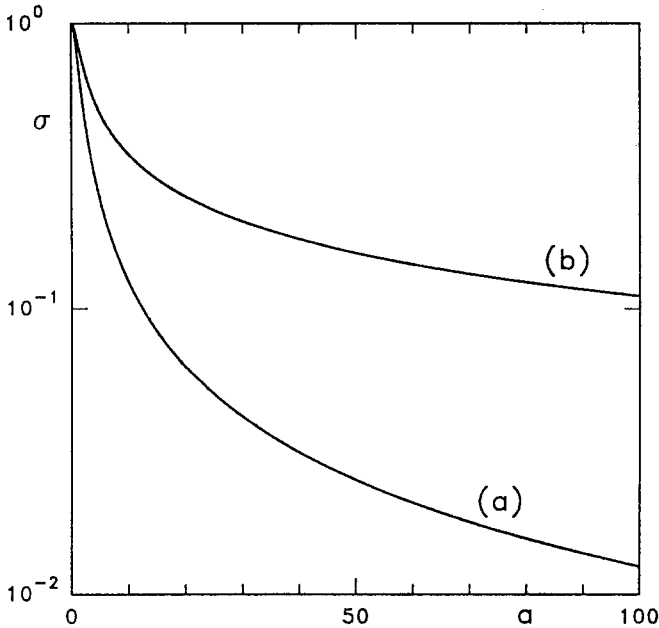


Fig. 1. Angular frequency σ as a function of amplitude a ; (a) for potential V_1 ; (b) for potential V_2 .

As the amplitude is increased, the convergence of these series becomes slower and finally the series diverge. Two simple techniques are used to overcome this problem: a change of variables (use of the energy instead of the amplitude) and the replacement of power series by equivalent continued fractions (see for instance Khovanskii 1963). The use of these two techniques give excellent results. For example, the terms of the series giving σ have alternate signs and slowly decreasing absolute values. The convergence becomes very slow as the amplitude approaches unity and the series diverges for amplitudes greater than unity. The equivalent continued fraction

$$\sigma = \frac{1}{1 + \frac{\sigma'_1 E}{1 + \frac{\sigma'_2 E}{1 + \frac{\sigma'_3 E}{1 + \frac{\sigma'_4 E}{\dots}}}}} \quad (15)$$

is computed analytically from the power series with REDUCE. The rational coefficients σ'_i are then converted in real format and used in a FORTRAN or Pascal program to produce numerical values of σ . Figure 1 shows σ as a function of the amplitude a obtained analytically. Figure 2 gives the number of terms (not counting the term of order zero) of the continued fraction necessary to obtain a given precision. Of course the computation of the angular frequency is not the goal of our study and may be achieved by simpler means.

The same technique may be applied to the series giving $x(t)$. One obtains a rational fraction the terms of which are Fourier series. Contopoulos and Seimenis (1990) have used similar expressions as the starting point of their study of orbits in a two-dimensional logarithmic potential.

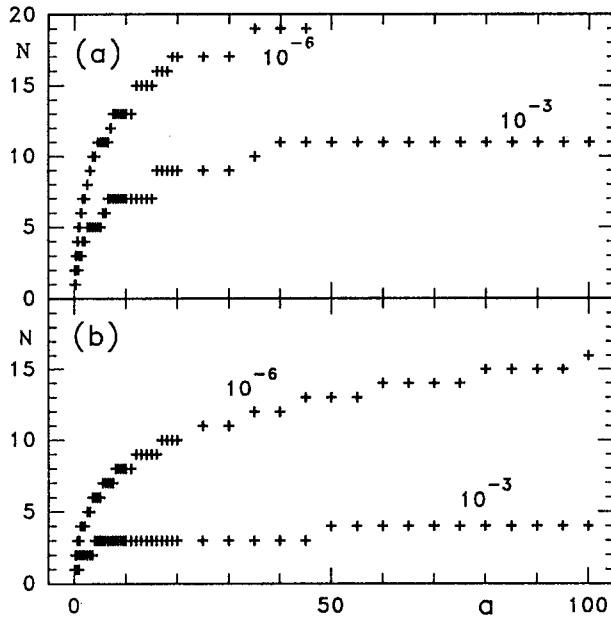


Fig. 2. Number of terms of the continued fractions necessary to achieve a given accuracy in $\sigma(a)$; (a) for potential V_1 ; (b) for potential V_2 .

4. Stability of the Motion

4.1. NUMERICAL COMPUTATION

We describe briefly the numerical method used to validate our analytical results. The use of Poincaré sections is widespread for the study of dynamical systems with two degrees of freedom. It has been explained by several authors: Hadjidemetriou (1975), Hénon (1976), Magneat (1982 and 1982b), Pfenniger (1984). The phase space of such a system is of dimension 4. Imposing the value of the energy integral, the points of the plane of section $x = 0$ can be located by two coordinates y and \dot{y} . Let P be the intersection of an orbit and the surface of section and TP , T^2P , \dots the successive intersections (to remove the sign ambiguity in \dot{x} , the points are plotted in the surface of section only when $\dot{x} > 0$). The Poincaré's application T is symplectic (area preserving), the justifications can be found in Binney et al. (1985). The stability of the motion along the x -axis reduces to the study of the stability of the origin of the plane of section as a fixed point of the Poincaré's application. When computing the motion along the x -axis, we compute at the same time the solutions of the variational equations, from which one obtains easily the linear operator T' , derivative of the map T . It is obtained as a two-dimensional square matrix. The origin, fixed point of the Poincaré map, is stable if the modulus

of eigenvalues of this matrix are less than unity. As T' is symplectic, $\det T' = 1$ and the characteristic equation is

$$\lambda^2 - \lambda \operatorname{tr} T' + 1 = 0, \quad (16)$$

where $\operatorname{tr} T'$ means the trace of the matrix. The condition of stability reduces to

$$|\operatorname{tr} T'| < 2. \quad (17)$$

In the plane of the parameters (q, a) , the stability boundary is given by

$$|\operatorname{tr} T'| = 2. \quad (18)$$

4.2. ANALYTICAL COMPUTATION

Consider a motion in the neighbourhood of the x -axis. The linearized equations are (y is infinitely small, but x is not)

$$\ddot{x} + 2x f'(1 + x^2) = 0, \quad (19)$$

$$\ddot{y} + 2y f'(1 + x^2)/q^2 = 0. \quad (20)$$

The z -perturbation would satisfy an equation of the same form as Equation (20). These equations are decoupled and this circumstance allows us to study separately the y and z component of the perturbation, reducing the stability problem to a two-dimensional one. Equation (19) is the same as Equation (9), its solution has been obtained in the preceding section. Equation (20) is of the form

$$\ddot{y} + \omega^2(t)y = 0. \quad (21)$$

As $x(t)$ is a periodic function with angular frequency σ and $\omega^2(t)$ is a function of x^2 , $\omega^2(t)$ is a periodic function of angular frequency 2σ . The problem reduces to the study of the stability of the equilibrium position of a parametric oscillator. This approach has already been used by Pfenniger (1987), in the case of models with figure rotation. Parametric excitation is studied in mechanics textbooks (for instance, Arnold 1976). When $\omega^2(t)$ is a mere sine function of time, Equation (21) reduces to Mathieu's equation. The stability boundaries in the space of the parameters (usually the frequency and the amplitude of the modulation) are determined by the characteristic values of Mathieu's equation. This equation has already been used in the study of stability of galactic orbits (Binney 1978 and Heiligman and Schwarzschild 1979).

In the present case, $\omega^2(t)$ is not a sine function of t and Equation (21) is a Hill's equation. Nevertheless, if we use the known results about the classical parametric oscillator, we expect the existence, in the plane of the parameters (q, a) , of a denumerable infinity of instability zones, touching the q -axis when $\omega = k\sigma$ with k integer (no divisor 2 in our case as the modulation frequency of ω^2 is 2σ), that is

for $q = 1/k$. In the following, we study the first two unstable zones, which arise, for small amplitudes, when q is close to 1 and $1/2$ respectively. It is known that the width of the unstable zone is a decreasing function of k . Moreover, smaller values of q are of lesser interest for galactic dynamics.

Let $s = \sigma t$. Substituting for $x(t)$ the expression obtained in the preceding section, Equation (21) becomes

$$q^2 d^2y/ds^2 + h(s)y = 0 , \tag{22}$$

where

$$h(s) = 2f'(1 + x^2)/\sigma^2 . \tag{23}$$

We develop $h(s)$ in series of $\epsilon = a^2$ and obtain an expression of the following form:

$$\begin{aligned} h(s) &= 1 + \epsilon(h_{10} + h_{11} \cos 2s) + \epsilon^2(h_{20} + h_{21} \cos 2s + h_{22} \cos 4s) \\ &\quad + \epsilon^3(h_{30} + h_{31} \cos 2s + h_{32} \cos 4s + h_{33} \cos 6s) + \dots \\ &= H_0 + H_1 \cos 2s + H_2 \cos 4s + H_3 \cos 6s + \dots , \end{aligned} \tag{24}$$

where

$$H_0 = 1 + \epsilon h_{10} + \epsilon^2 h_{20} + \epsilon^3 h_{30} + \dots = O(1) , \tag{25}$$

$$H_1 = \epsilon h_{11} + \epsilon^2 h_{21} + \epsilon^3 h_{31} + \dots = O(\epsilon) , \tag{26}$$

$$H_2 = \epsilon^2 h_{22} + \epsilon^3 h_{32} + \dots = O(\epsilon^2) , \tag{27}$$

$$H_3 = \epsilon^3 h_{33} + \dots = O(\epsilon^3) . \tag{28}$$

We study Hill's equation in the same way as Mathieu's equation (see Ince 1956). When the point (q, a) is on a stability boundary, Equation (22) has a periodic solution which is either even or odd. Let a_k denote a boundary corresponding to an even periodic solution and b_k denote a boundary corresponding to an odd solution. This notation agrees with that used by Abramowitz and Stegun (1968) for the characteristic values of Mathieu's equation. The boundaries a_k and b_k touch the q -axis at $q = 1/k$. The angular frequency of a periodic solution is σ if k is odd and 2σ if k is even. The justification of these statements are the same as that used in the study of Mathieu's equation (Ince 1956). In the following, the determination of the periodic solutions of Equation (22) will give us the boundaries a_1, b_1, a_2 and b_2 .

To determine the a_1 -boundary, one seeks a periodic solution of the form

$$y = \sum_{n=0}^{\infty} y_n \cos(2n + 1)s . \tag{29}$$

We substitute this expression for y in Equation (22). It comes out

$$\sum_{l=0}^{\infty} A_{kl} y_l = 0 , \quad (k = 0, 1, 2, \dots) , \tag{30}$$

with

$$A_{kk} = -(2k + 1)^2 q^2 + H_0 + \frac{1}{2} H_{2k+1} \tag{31}$$

$$A_{kl} = \frac{1}{2} H_{|k-l|} + \frac{1}{2} H_{k+l+1}, \quad (k \neq l). \tag{32}$$

We must now express that this system admits a non vanishing solution. In the case of Mathieu’s equation, the system is tridiagonal and this condition may be written as the vanishing of a continued fraction. This process cannot be adapted to our case. Let D_n be the determinant of the matrix A of the coefficients A_{kl} with indices $k, l \leq n$. We consider successively the equations

$$D_0 = 0, D_1 = 0, \dots, D_n = 0, \tag{33}$$

and we make the substitution

$$q = 1 + \delta. \tag{34}$$

Then these equations are solved for δ , the solutions being expressed as power series of ϵ . It turns out that the solution of $D_k = 0$ coincide with the solution of $D_l = 0$ with $l > k$ up to order $2k + 1$. This can be proved rigourously, but the proof is long and tedious. In fact, the success of this process rests on the fact that the elements of the matrix A are decreasing when moving away from the principal diagonal,

$$A_{kl} = O(\epsilon^{|k-l|}). \tag{35}$$

One proceeds in the same way for the other stability boundaries. We write only the major steps of the calculation. For the b_1 -boundary, we have

$$y = \sum_{n=0}^{\infty} y_n \sin(2n + 1)s. \tag{36}$$

$$\sum_{l=0}^{\infty} A_{kl} y_l = 0, \quad (k = 0, 1, 2, \dots), \tag{37}$$

with

$$A_{kk} = -(2k + 1)^2 q^2 + H_0 - \frac{1}{2} H_{2k+1}, \tag{38}$$

$$A_{kl} = \frac{1}{2} H_{|k-l|} - \frac{1}{2} H_{k+l+1}, \quad (k \neq l). \tag{39}$$

For the a_2 -boundary, we write

$$y = \sum_{n=0}^{\infty} y_n \cos 2ns. \tag{40}$$

$$\sum_{l=0}^{\infty} A_{kl} y_l = 0, \quad (k = 0, 1, 2, \dots), \quad (41)$$

with

$$A_{00} = 2H_0, \quad (42)$$

$$A_{kk} = -4q^2 k^2 + H_0 + \frac{1}{2} H_{2k}, \quad (k > 0), \quad (43)$$

$$A_{kl} = \frac{1}{2} H_{|k-l|} + \frac{1}{2} H_{k+l}, \quad (k \neq l). \quad (44)$$

We put

$$q = \frac{1}{2} + \delta. \quad (45)$$

Here, we have

$$D_0 = 2 + O(\epsilon) \quad (46)$$

and the characteristic equation cannot be solved for $k = 0$. The power series obtained from $D_k = 0$ gives the solution up to order $2k - 1$.

For the b_2 -boundary,

$$y = \sum_{n=1}^{\infty} y_n \sin 2ns. \quad (47)$$

$$\sum_{l=1}^{\infty} A_{kl} y_l = 0, \quad (k = 1, 2, \dots), \quad (48)$$

with

$$A_{kk} = -4q^2 k^2 + H_0 - \frac{1}{2} H_{2k}, \quad (49)$$

$$A_{kl} = \frac{1}{2} H_{|k-l|} - \frac{1}{2} H_{k+l}, \quad (k \neq l). \quad (50)$$

With δ defined as in Equation (45), the power series obtained from $D_k = 0$ gives the solution up to order $2k - 1$.

At all orders, the a_1 -boundary is given exactly by $q = 1$. This means that for q close to unity, orbits along the long axis are stable and orbits along the short axis are unstable, as it is well-known. For the other boundaries, we have obtained the expressions of q as power series up to the terms of order 18:

$$q = q_0 + q_1 \epsilon + q_2 \epsilon^2 + q_3 \epsilon^3 + q_4 \epsilon^4 + \dots. \quad (51)$$

As was expected, the second unstable zone is narrower than the first one: the width of the first zone is of the order of a^2 whereas the width of the second one is of the order of a^4 .

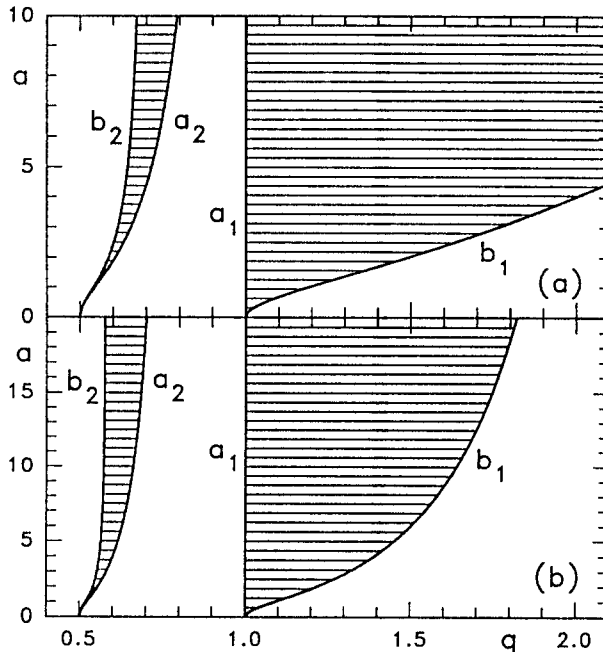


Fig. 3. Unstable zones (shaded areas) for the motion along the x -axis in the plane of the parameters (q, a) ; (a) for potential V_1 ; (b) for potential V_2 .

Again, the power series are not of great practical use when the amplitude is not markedly smaller than unity. We obtain a satisfactory convergence if we express the series in terms of the energy and convert them into continued fractions:

$$q = \frac{q'_0}{1+} \frac{q'_1 E}{1+} \frac{q'_2 E}{1+} \frac{q'_3 E}{1+} \frac{q'_4 E}{1+} \dots \tag{52}$$

The results are shown in Figure 3. The first few terms, for both potentials, are given in the appendices. Figures 4 and 5 show the number of terms (not counting the term of order zero) necessary to obtain a given accuracy in $q(a)$.

5. The Organization of the Main Families of Orbits in the Plane

The results obtained for x -axis orbits for $q > 1$ are now interpreted in terms of y -axis orbits with a shape parameter $1/q$. For a y -axis orbit, a is no longer the amplitude and must be interpreted as a measure of the energy (the amplitude of a y -axis orbit is qa). This gives Figure 6, which differs from Figure 3 only by the drawing of the b_1 -boundary which separates regions of stability (below) and instability (above) of y -axis orbits. The different stability boundaries we have considered here determine six regions in the plane of the parameters. We use Roman numerals to number them.

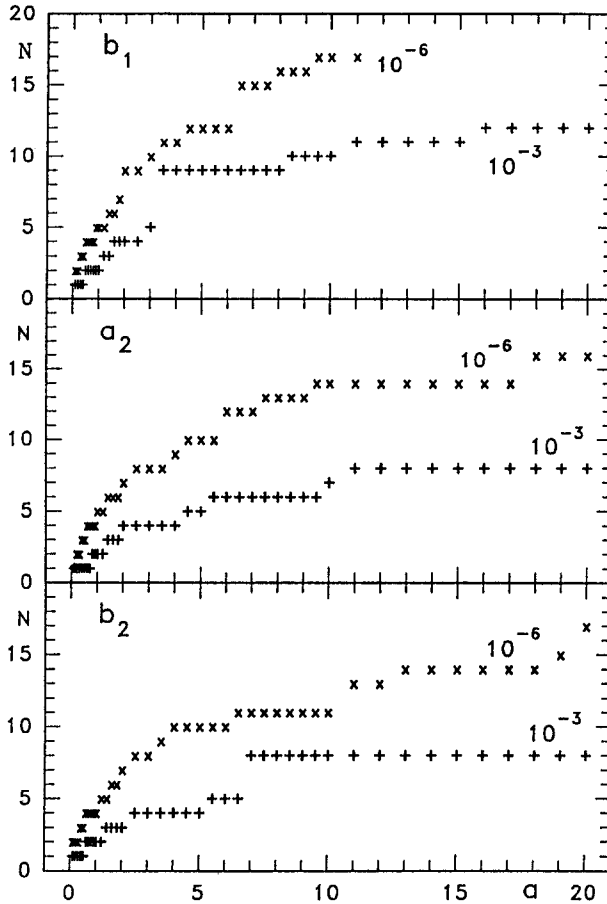


Fig. 4. Number of terms of the continued fractions necessary to achieve a given accuracy in $q(a)$ for potential V_1 .

Miralda-Escudé and Schwarzschild (1989) have studied motions along the axes in a logarithmic potential with notations slightly different of ours. Their parameter b is the same as our q and their parameter R_c decreases as our a increases. Their bifurcation diagrams (their Figures 6 and 7) show, for fixed q values, the appearance of instabilities of the axis orbits and the simultaneous appearance of new orbit families.

Our results are similar. As only stable periodic orbits can parent a family of orbits, the partition of the plane (q, a) according to the stability properties of axis orbits also corresponds to different organizations of the orbits in the (x, y) -plane into main families. New families of orbits appear when we cross the stability boundaries of Figure 6. Table I shows, for the six regions, the stability of the axial orbits and the main families of orbits. We use the notation B for the box orbits, whose parents are the stable axis orbits. When necessary, we add the index x or y to indicate the parent orbit. The banana orbits are marked Ba , they appear when the

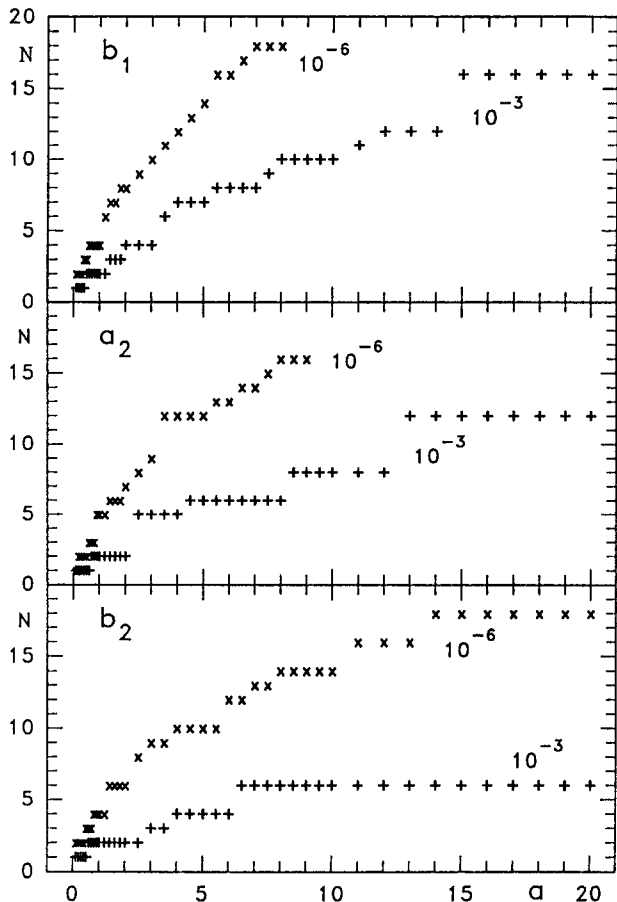


Fig. 5. Number of terms of the continued fractions necessary to achieve a given accuracy in $q(a)$ for potential V_2 .

x -axis orbit loses its stability. The loop orbits are marked L and appear when the y -axis orbit loses its stability. Finally in regions V and VI there exists a region of phase space occupied by box and boxlets that we have designated as B' . The same notations have been used in Figures 6 to 11. They show Poincaré sections ($x = 0$), computed numerically, for values of the parameters chosen in the six regions.

The narrowing of the stability domains as the energy increases is linked to the disappearance of box orbits in potential V_1 observed by Miralda-Escudé and Schwarzschild (1989) as $E \rightarrow \infty$ (as $R_c \rightarrow 0$ in their notations). This disappearance of the box orbits does not seem to be linked to a particular form of the potential (de Zeeuw and Pfenniger 1988, Lees and Schwarzschild 1992).

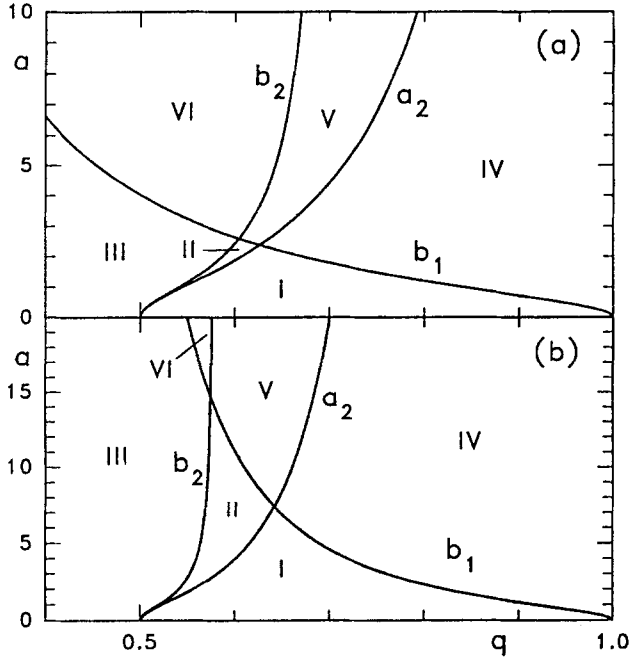


Fig. 6. The stability boundaries divide the plane of the parameters (q, a) into six regions ; (a) for potential V_1 ; (b) for potential V_2

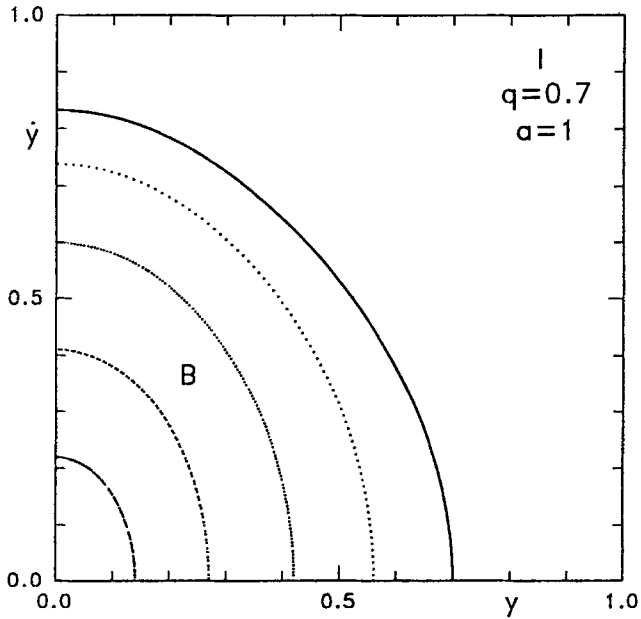


Fig. 7. Poincaré section $x = 0$ for potential V_1 and (q, a) chosen in region I.

TABLE I

The + or - signs indicate stability or instability respectively of the axial orbits. Refer to the text for the description of the main families of orbits.

Zone	x -orbit	y -orbit	Main families
I	+	+	B
II	-	+	B_y , Ba
III	+	+	B_x , B_y , Ba
IV	+	-	B_x , L
V	-	-	Ba, L, B'
VI	+	-	B_x , Ba, L, B'

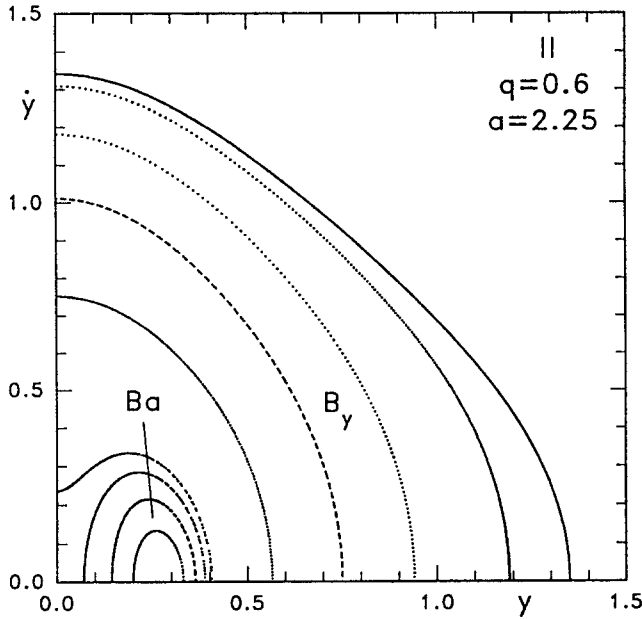


Fig. 8. Poincaré section $x = 0$ for potential V_1 and (q, a) chosen in region II.

6. Conclusions

The instability of axial orbits when their frequencies are close to resonances is of the same nature as the parametric instability, well studied in mechanics textbooks. We have shown that the boundaries of this instability in the space of the parameters (the ellipticity and the energy) can be entirely determined by analytical methods. In principle, the power series developments used in this work can be carried

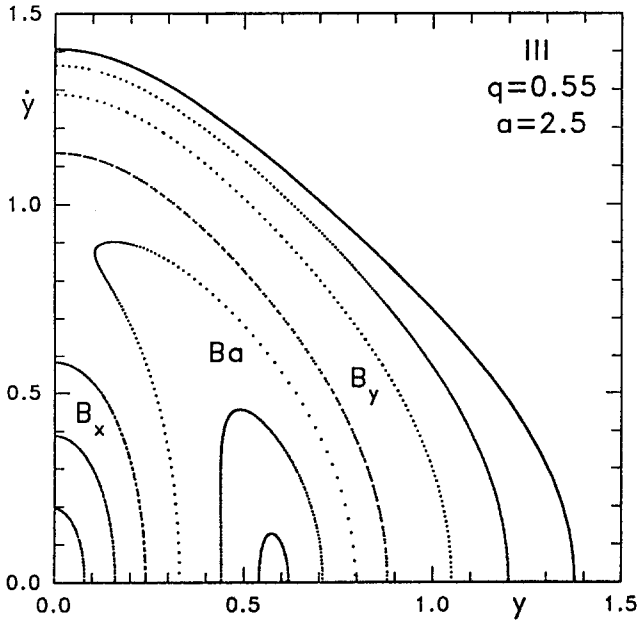


Fig. 9. Poincaré section $x = 0$ for potential V_1 and (q, a) chosen in region III.

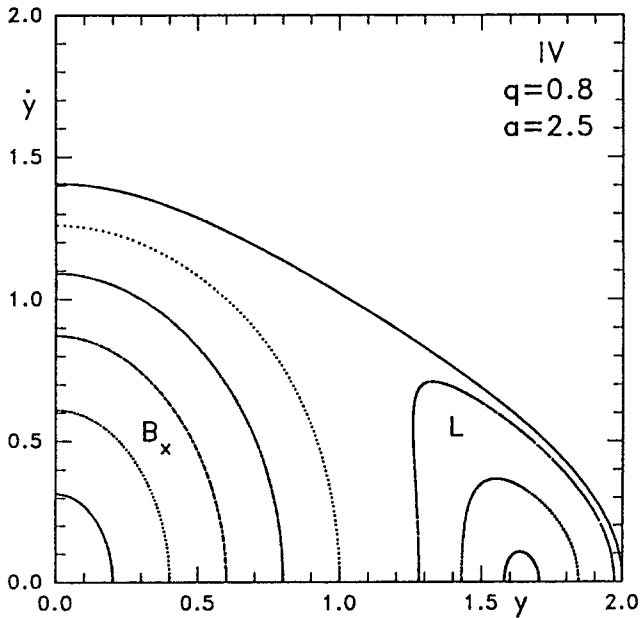


Fig. 10. Poincaré section $x = 0$ for potential V_1 and (q, a) chosen in region IV.

out up to an arbitrary order. They are only limited by the available computing power. An elementary summation process (change of variables and transformation

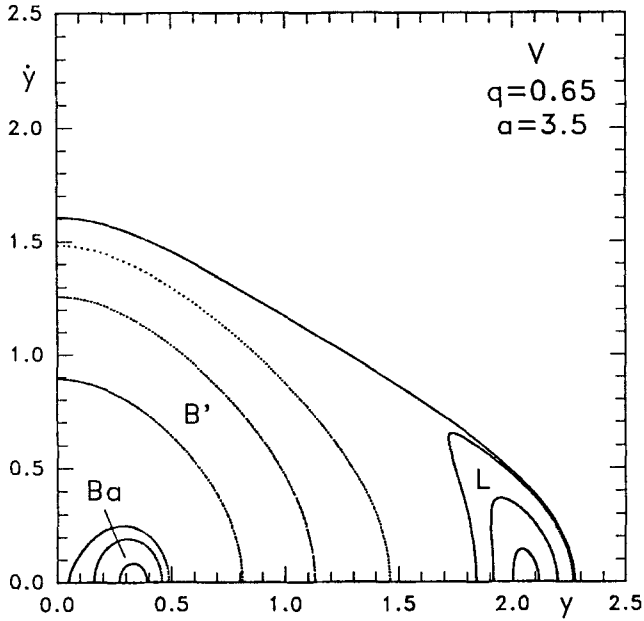


Fig. 11. Poincaré section $x = 0$ for potential V_1 and (q, a) chosen in region V.

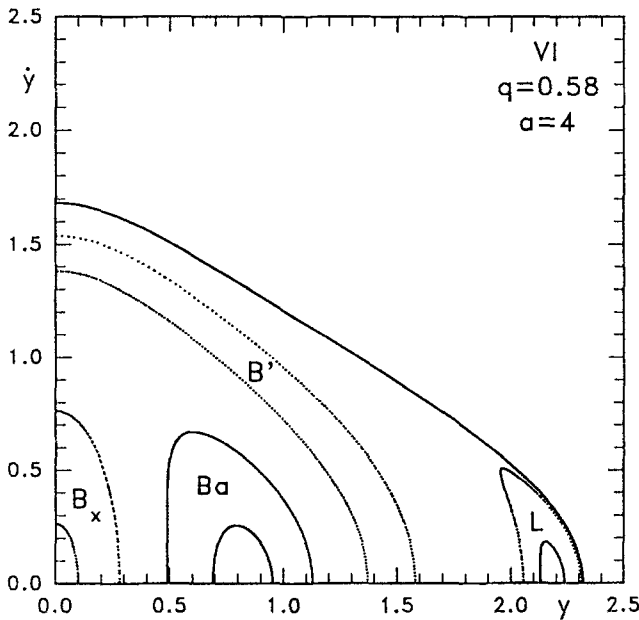


Fig. 12. Poincaré section $x = 0$ for potential V_1 and (q, a) chosen in region VI.

into continued fractions) allows the use of the analytical results well beyond the relatively narrow domain of convergence of the power series.

Of course, the analytical method is limited to the study of analytical potentials. And it requires a computer as numerical computation does. We insist on the simplicity of the analytical method used in this work. Future investigations will tell us if this method can be used in more complex situations.

The knowledge of the stability of axial orbits allows the partition of the space of parameters (q, a) in regions corresponding to different organizations of the main families of orbits in the (xy) -plane. Only the existence of the main families, parented by axial orbits (box orbits) or stemming from their instability (banana orbits and loop orbits) can be localized in the parameter space. Families stemming from further bifurcations escape our analysis. The same approach for the three-dimensional problem should provide the same type of information about the organization of the main families in three-dimensional space. However, the parameter space would be three-dimensional (energy and two ellipticity parameters) and the results would be more difficult to visualize.

Acknowledgements

We are grateful to the Belgian Fonds National de la Recherche Scientifique who supported this work. It is a pleasure to thank P. O. Vandervoort whose comments help us to improve the manuscript.

Appendix

A. Potential V_1

In this appendix, we give the expressions obtained for the logarithmic potential $V_1(x, y)$ described by Equation (2). As the writing of the coefficients becomes rapidly cumbersome as the order increases, we truncate the expressions and tables at relatively low orders.

$$F(x) = -x^3 + x^5 - x^7 + x^9 - x^{11} + x^{13} - \dots \quad (53)$$

$$E = \frac{1}{2}\epsilon - \frac{1}{4}\epsilon^2 + \frac{1}{6}\epsilon^3 - \frac{1}{8}\epsilon^4 + \frac{1}{10}\epsilon^5 - \frac{1}{12}\epsilon^6 + \dots \quad (54)$$

$$\epsilon = 2E + 2E^2 + \frac{4}{3}E^3 + \frac{2}{3}E^4 + \frac{4}{15}E^5 + \frac{4}{45}E^6 + \frac{8}{315}E^7 + \dots \quad (55)$$

$$\begin{aligned} \sigma = 1 - \frac{3}{8}\epsilon + \frac{59}{256}\epsilon^2 - \frac{337}{2048}\epsilon^3 + \frac{99745}{786432}\epsilon^4 \\ - \frac{3224423}{31457280}\epsilon^5 + \frac{258427301}{3019898880}\epsilon^6 - \frac{1374782873}{8790481920}\epsilon^7 + \dots \end{aligned} \quad (56)$$

$$\begin{aligned}
 x/a = & \cos s + \epsilon \left(\frac{1}{32} \cos s - \frac{1}{32} \cos 3s \right) + \epsilon^2 \left(-\frac{59}{3072} \cos s + \frac{1}{64} \cos 3s \right. \\
 & \left. + \frac{11}{3072} \cos 5s \right) + \epsilon^3 \left(\frac{1313}{98304} \cos s - \frac{149}{16384} \cos 3s - \frac{15}{4096} \cos 5s \right. \\
 & \left. - \frac{59}{98304} \cos 7s \right) + \epsilon^4 \left(-\frac{234967}{23592960} \cos s + \frac{18229}{3145728} \cos 3s \right. \\
 & \left. + \frac{4901}{1572864} \cos 5s + \frac{547}{589824} \cos 7s + \frac{1903}{15728640} \cos 9s \right) + \dots \quad (57)
 \end{aligned}$$

The coefficients of the continued fraction describing σ as a function of E are given in Table II.

TABLE II
Coefficients of the continued fraction giving σ , Equation (15).

i	σ'_i
1	3/4
2	-25/48
3	41/240
4	-693/3280
5	18769/108240
6	-174373/1519056
7	3233205943/14683057200

$$\begin{aligned}
 h = & 1 + \epsilon \left(\frac{1}{4} - \frac{1}{2} \cos 2s \right) + \epsilon^2 \left(-\frac{9}{128} + \frac{1}{8} \cos 2s + \frac{5}{32} \cos 4s \right) \\
 & + \epsilon^3 \left(\frac{55}{1536} - \frac{335}{6144} \cos 2s - \frac{23}{192} \cos 4s - \frac{313}{6144} \cos 6s \right) \\
 & + \epsilon^4 \left(-\frac{8839}{393216} + \frac{239}{8192} \cos 2s + \frac{353}{4096} \cos 4s + \frac{537}{8192} \cos 6s \right. \\
 & \left. + \frac{277}{16384} \cos 8s \right) + \dots \quad (58)
 \end{aligned}$$

$$\begin{aligned}
 q_{b1} = & 1 + \frac{1}{4}\epsilon - \frac{3}{32}\epsilon^2 + \frac{41}{768}\epsilon^3 - \frac{293}{8192}\epsilon^4 + \frac{19297}{737280}\epsilon^5 \\
 & - \frac{5733503}{283115520}\epsilon^6 + \frac{3098381807}{190253629440}\epsilon^7 - \dots \quad (59)
 \end{aligned}$$

TABLE III

Coefficients of the continued fraction giving $q(E)$, for the b_1 -boundary, Equation (52).

i	q'_i
0	1
1	-1/2
2	1/4
3	-1/6
4	31/96
5	-391/4960
6	33974/181815
7	-262826339/2975578816

TABLE IV

Coefficients of the continued fraction giving $q(E)$, for the a_2 -boundary, Equation (52).

i	q'_i
0	1/2
1	-1/4
2	7/48
3	-109/336
4	11629/36624
5	-31875431/304214640
6	2852486221567/12709007557680
7	-151507989929326679/817143405960019056

$$q_{a2} = \frac{1}{2} + \frac{1}{16}\epsilon - \frac{43}{1536}\epsilon^2 + \frac{209}{12288}\epsilon^3 - \frac{167849}{14155776}\epsilon^4 + \frac{5062619}{566231040}\epsilon^5 - \frac{2313264119}{326149079040}\epsilon^6 + \frac{106474807777}{18264348426240}\epsilon^7 - \dots \quad (60)$$

$$q_{b2} = \frac{1}{2} + \frac{1}{16}\epsilon - \frac{55}{1536}\epsilon^2 + \frac{301}{12288}\epsilon^3 - \frac{258905}{14155776}\epsilon^4 + \frac{8154379}{566231040}\epsilon^5 - \frac{766778089}{65229815808}\epsilon^6 + \frac{179892123427}{18264348426240}\epsilon^7 - \dots \quad (61)$$

TABLE V
Coefficients of the continued fraction giving $q(E)$, for the b_2 -boundary, Equation (52).

i	q'_i
0	1/2
1	-1/4
2	19/48
3	-181/912
4	36865/165072
5	-144182963/1601415600
6	5720036896171/67140693865200
7	-39437947844746780235/80578629747458776752

Tables III, IV and V give the coefficients of the continued fractions describing q on the stability boundaries as functions of E .

B. Potential V_2

We now consider the potential $V_2(x, y)$ defined by Equation (3). We have obtained the following expressions.

$$F(x) = -\frac{1}{2}x^3 + \frac{3}{8}x^5 - \frac{5}{16}x^7 + \frac{35}{128}x^9 - \frac{63}{256}x^{11} + \frac{231}{1024}x^{13} - \frac{429}{2048}x^{15} + \dots \quad (62)$$

$$E = \frac{1}{2}\epsilon - \frac{1}{8}\epsilon^2 + \frac{1}{16}\epsilon^3 - \frac{5}{128}\epsilon^4 + \frac{7}{256}\epsilon^5 - \frac{21}{1024}\epsilon^6 + \frac{33}{2048}\epsilon^7 - \dots \quad (63)$$

$$\epsilon = 2E + E^2. \quad (64)$$

$$\begin{aligned} \sigma = 1 - \frac{3}{16}\epsilon + \frac{99}{1024}\epsilon^2 - \frac{1025}{16384}\epsilon^3 + \frac{188955}{4194304}\epsilon^4 \\ - \frac{2319273}{67108864}\epsilon^5 + \frac{118774401}{4294967296}\epsilon^6 - \frac{1567395747}{68719476736}\epsilon^7 + \dots \end{aligned} \quad (65)$$

$$\begin{aligned} x/a = \cos s + \epsilon \left(\frac{1}{64} \cos s - \frac{1}{64} \cos 3s \right) + \epsilon^2 \left(-\frac{41}{4096} \cos s \right. \\ \left. + \frac{9}{1024} \cos 3s + \frac{5}{4096} \cos 5s \right) + \epsilon^3 \left(\frac{1887}{262144} \cos s \right. \end{aligned}$$

$$\begin{aligned}
& -\frac{747}{131072} \cos 3s - \frac{265}{196608} \cos 5s - \frac{119}{786432} \cos 7s \Big) \\
& + \epsilon^4 \left(-\frac{46369}{8388608} \cos s + \frac{67395}{16777216} \cos 3s + \frac{31195}{25165824} \cos 5s \right. \\
& \left. + \frac{3115}{12582912} \cos 7s + \frac{393}{16777216} \cos 9s \right) + \dots \tag{66}
\end{aligned}$$

The coefficients of the continued fraction describing σ as a function of E are given in Table VI.

TABLE VI

Coefficients of the continued fraction giving σ , Equation (15).

i	σ'_i
1	3/8
2	5/32
3	13/96
4	161/1248
5	6083/47840
6	404001/3197920
7	197478759/1568343392

TABLE VII

Coefficients of the continued fraction giving $q(E)$, for the b_1 -boundary, Equation (52).

i	q'_i
0	1
1	-1/4
2	5/8
3	1/20
4	69/320
5	-85/4416
6	1874/391
7	-133302503/36700416

TABLE VIII

Coefficients of the continued fraction giving $q(E)$, for the a_2 -boundary, Equation (52).

i	q'_i
0	1/2
1	-1/8
2	43/96
3	59/4128
4	-117001/243552
5	966352975/662693664
6	-258792295751497/1262112719196000
7	3137849198471454849551/47315986738328227668000

TABLE IX

Coefficients of the continued fraction giving $q(E)$, for the b_2 -boundary, Equation (52).

i	q'_i
0	1/2
1	-1/8
2	79/96
3	-157/7584
4	292933/1190688
5	941605661/4415086176
6	1285176440343637/1675913140822560
7	-70334480586313695557/2754846396618800691360

$$\begin{aligned}
 h = & 1 + \epsilon \left(\frac{1}{8} - \frac{1}{4} \cos 2s \right) + \epsilon^2 \left(-\frac{25}{512} + \frac{3}{32} \cos 2s + \frac{7}{128} \cos 4s \right) \\
 & + \epsilon^3 \left(\frac{113}{4096} - \frac{829}{16384} \cos 2s - \frac{25}{512} \cos 4s - \frac{219}{16384} \cos 6s \right) \\
 & + \epsilon^4 \left(-\frac{38317}{2097152} + \frac{4205}{131072} \cos 2s + \frac{7769}{196608} \cos 4s \right. \\
 & \left. + \frac{2475}{131072} \cos 6s + \frac{2701}{786432} \cos 8s \right) + \dots
 \end{aligned} \tag{67}$$

$$q_{b1} = 1 + \frac{1}{8}\epsilon - \frac{7}{128}\epsilon^2 + \frac{67}{2048}\epsilon^3 - \frac{2941}{131072}\epsilon^4 + \frac{8721}{524288}\epsilon^5 - \frac{5222323}{402653184}\epsilon^6 + \frac{810101701}{77309411328}\epsilon^7 - \dots \quad (68)$$

$$q_{a2} = \frac{1}{2} + \frac{1}{32}\epsilon - \frac{79}{6144}\epsilon^2 + \frac{239}{32768}\epsilon^3 - \frac{1087769}{226492416}\epsilon^4 + \frac{12504287}{3623878656}\epsilon^5 - \frac{54803269409}{20873541058560}\epsilon^6 + \frac{694872636193}{333976656936960}\epsilon^7 - \dots \quad (69)$$

$$q_{b2} = \frac{1}{2} + \frac{1}{32}\epsilon - \frac{115}{6144}\epsilon^2 + \frac{427}{32768}\epsilon^3 - \frac{2224937}{226492416}\epsilon^4 + \frac{28199471}{3623878656}\epsilon^5 - \frac{133116169379}{20873541058560}\epsilon^6 + \frac{1789448743963}{333976656936960}\epsilon^7 - \dots \quad (70)$$

Tables VII, VIII and IX give the coefficients of the continued fractions describing q on the stability boundaries as functions of E .

References

- Abramowitz, M., Stegun, I.: 1968, *Handbook of Mathematical Functions*, 7th edition, National Bureau of Standards.
- Arnold, V.: 1976, *Les méthodes mathématiques de la mécanique classique*, Editions Mir, Moscou.
- Binney, J.: 1978, *Mon. Not. R. astr. Soc.* **183**, 779.
- Binney, J.: 1981, *Mon. Not. R. astr. Soc.* **196**, 455.
- Binney, J., Gerhard, E.O., Hut, P.: 1985, *Mon. Not. R. astr. Soc.* **215**, 59.
- Binney, J., Tremaine, S.: 1987, *Galactic Dynamics*, Princeton University Press.
- Contopoulos, G., Seimenis, J.: 1990, *Astron. Astrophys.* **227**, 49.
- Davoust, E.: 1983, *Astron. Astrophys.* **125**, 101.
- Gerhard, O.E., Binney, J.: 1985, *Mon. Not. R. astr. Soc.* **216**, 467.
- Goodman, J., Schwarzschild, M.: 1981, *Astrophys. J.* **245**, 1087.
- Hadjidemetriou, J.D.: 1975, *Celest. Mech.* **12**, 255.
- Hayashi, C.: 1985, *Nonlinear Oscillations in Physical Systems*, Princeton University Press.
- Heiligman, G., Schwarzschild, M.: 1979, *Astrophys. J.* **233**, 872.
- Hénon, M.: 1976, *Celest. Mech.* **13**, 267.
- Ince, E.L.: 1956, *Ordinary Differential Equations*, Dover.
- Khovanskii, A.N.: 1963, *The Application of Continued Fractions and their Generalizations to Problems in Approximation Theory*, Noordhoff, Groningen.
- Lake, G., Norman, C.: 1983, *Astrophys. J.* **270**, 51.
- Lees, J.F., Schwarzschild, M.: 1992, *Astrophys. J.* **384**, 491.
- Magenat, P.: 1982a, *Astron. Astrophys.* **108**, 89.
- Magenat, P.: 1982b, *Celest. Mech.* **28**, 319.
- Martinet, L., de Zeeuw, T.: 1988, *Astron. Astrophys.* **206**, 269.
- Martinet, L., Udry, S.: 1990, *Astron. Astrophys.* **235**, 69.
- Miralda-Escudé, J., Schwarzschild, M.: 1989, *Astrophys. J.* **339**, 752.
- Nayfeh, A.H.: 1973, *Perturbation methods*, Wiley & Sons, New York.
- Patsis, P.A., Zachilas, L.: 1990, *Astron. Astrophys.* **227**, 37.
- Pearce, F.R., Thomas, P.A.: 1991, *Mon. Not. R. astr. Soc.* **248**, 688.
- Pfenniger, D.: 1984, *Astron. Astrophys.* **134**, 374.

Pfenniger, D.: 1987, *Astron. Astrophys.* **180**, 79.

Pfenniger, D., de Zeeuw, T.: 1989, in *Dynamics of Dense Stellar Systems*, ed. D. Merritt, Cambridge University Press, p. 81.

Robe, H.: 1987, *Astron. Astrophys.* **182**, 202.

Udry, S., Martinet, L.: 1994, *Astron. Astrophys.* **281**, 314.

de Zeeuw, T.: 1985, *Mon. Not. R. astr. Soc.* **215**, 731.

de Zeeuw, T., Pfenniger, D.: 1988, *Mon. Not. R. astr. Soc.* **235**, 949.